

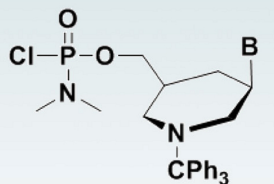
OL

Organic Letters

Volume 25, Issue 6

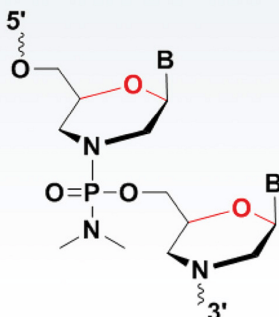
February 17, 2023

pubs.acs.org/ol

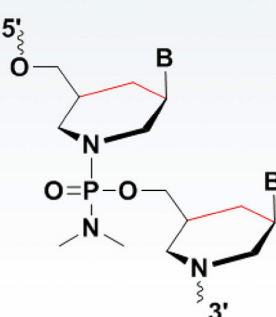


B = U, C^{Ac}, A^{Bz}; G^{i-Bu}

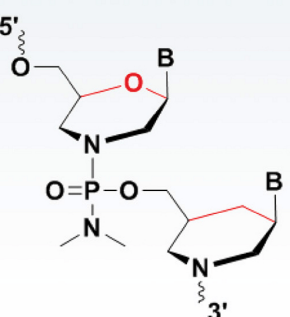
Chlorophosphoramide
Piperidino monomer



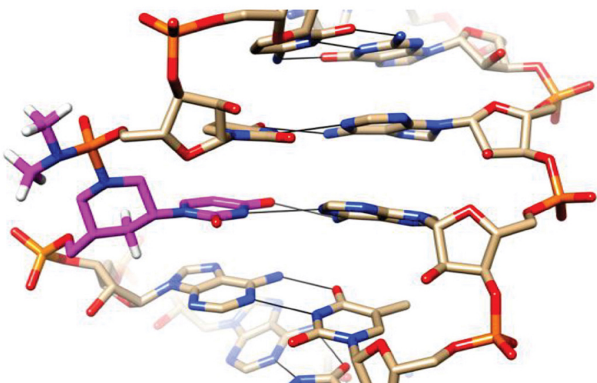
Phosphorodiamidate
Morpholino
Oligomer (PMO)



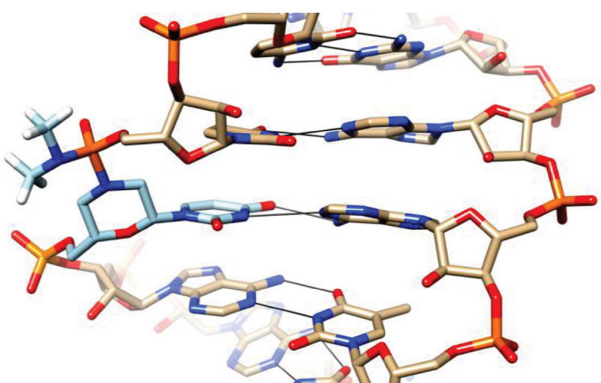
Piperidino
Phosphorodiamidate
Oligomer (PPO)



PMO-PPO
Chimera



Pip-U



PMO-U



ACS Publications
Most Trusted. Most Cited. Most Read.

www.acs.org

Synthesis and Biophysical Properties of Phosphorodiamidate Piperidino Oligomers

Atanu Ghosh,[†] Masaaki Akabane-Nakata,[†] Jayanta Kundu, Joel M. Harp, Mimouna Madaoui, Martin Egli, Muthiah Manoharan,* and Surajit Sinha*



Cite This: *Org. Lett.* 2023, 25, 901–906



Read Online

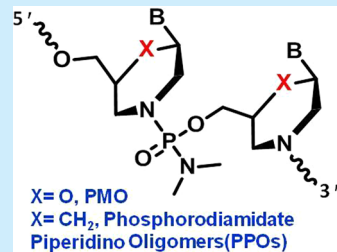
ACCESS |

Metrics & More

Article Recommendations

Supporting Information

ABSTRACT: We report the synthesis of piperidino nucleoside phosphoramidates functionalized with uracil, cytosine, guanine, and adenine and their incorporation into oligomers. High-performance liquid chromatography analyses demonstrated that a phosphorodiamidate piperidino oligomer (PPO) is more lipophilic than a phosphorodiamidate morpholino oligomer (PMO) of the same tetrameric sequence. A PMO containing piperidino residues formed duplexes with both DNA and RNA, and the PPO had higher stability at endosomal pH and higher hydrophobicity than the PMO.



Phosphorodiamidate morpholino oligomers (PMOs), which have a neutral backbone, were developed for use in oligonucleotide-based therapeutics.^{1,2} To date, four PMO-based drugs, eteplirsen, golodirsen, viltolarsen, and casimersen, have been approved by the U.S. Food and Drug Administration (FDA); these agents are used to treat patients with Duchenne muscular dystrophy.³ PMOs have also been shown to be effective against viral and bacterial infections and cancers in cell-based and preclinical models.^{4,5} In PMO, the five-membered ribose sugar unit of a natural nucleotide is replaced by a morpholino ring. Carbocyclic nucleosides, in which the furanose ring oxygen is replaced by a CH₂ group, have also been reported and have been approved as antitumor and antiviral therapies.^{2,6} Carbocyclic modifications of oligonucleotides enhance resistance against nuclease degradation and stabilize the glycosidic bond against hydrolytic cleavage.

PMOs must be chemically modified to improve cellular uptake and pharmacokinetics.^{7,8} Among the reported modifications, incorporation of a guanidinium linkage or guanidinium-functionalized nucleobase is notable.⁹ Sinha's group demonstrated the cell-penetrating and gene-silencing properties of self-transferring guanidinium morpholino-PMO chimeras in cell culture and zebrafish.^{9d} The Hayes group reported that triazole-linked morpholino-DNA chimeras are resistant to enzymatic degradation.¹⁰ Caruthers's group developed thiophosphoramidate morpholino oligomers and their phosphorothioate DNA chimeras.⁸ Recently, Borbás's group reported alkylamine-linked, cationic morpholino analogues.¹¹

Here, we report the synthesis of phosphorodiamidate piperidino oligomers (PPOs). The four piperidino nucleoside monomers, pip-A, pip-U, pip-G, and pip-C, and corresponding chlorophosphoramidate monomers were prepared (Figure 1A). These were incorporated into oligomers to evaluate the

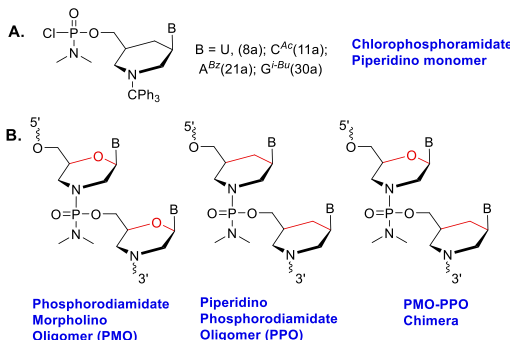


Figure 1. (A) Structure of chlorophosphoramidate piperidino monomers. (B) Structures of PMO and PPO and the PMO-PPO chimera.

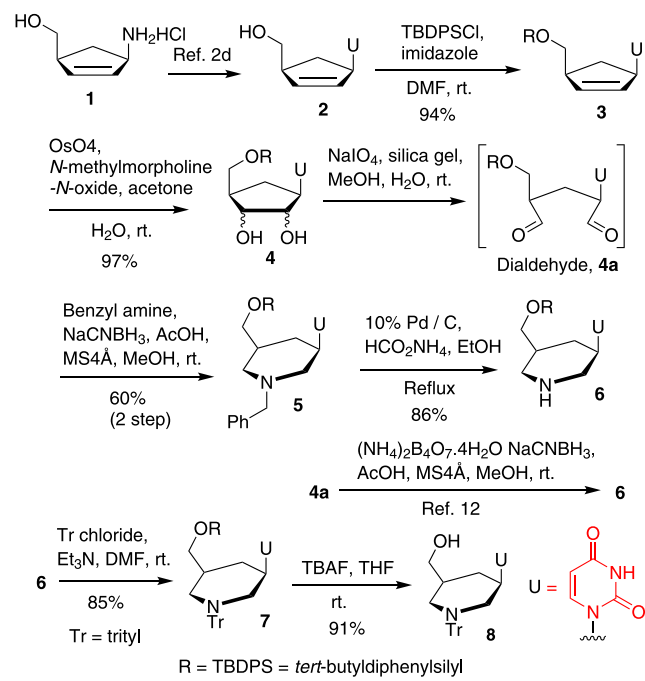
stability of their duplexes with DNA and RNA as well as their conformational properties using circular dichroism (CD) spectroscopy.

The pip monomers were synthesized from commercially available cyclopentenyl-amino-methanol 1. Car-U 2 was synthesized following the procedure previously reported for synthesis of carbocyclic RNA (Scheme 1).^{2c} Silyl protection and then double bond oxidation of compound 3 with OsO₄ gave diol 4. Diol cleavage by NaIO₄ and subsequent reductive cyclization with benzylamine gave N-benzyl pip-U monomer 5

Received: November 30, 2022

Published: February 3, 2023

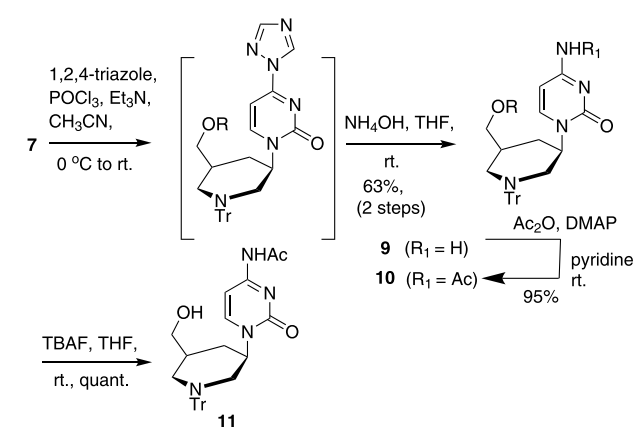


Scheme 1. Synthesis of Pip-U Monomer 8

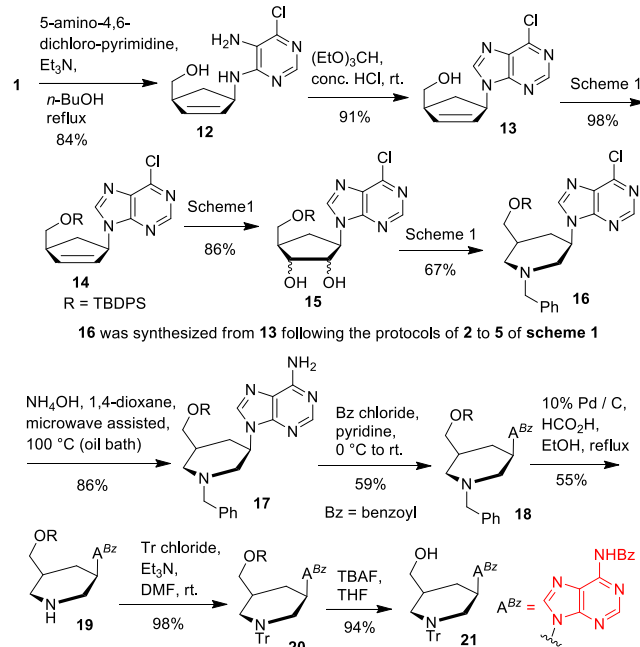
in 60% yield. Using $(\text{NH}_4)_2\text{B}_4\text{O}_7 \cdot 4\text{H}_2\text{O}$ as a nitrogen source as described previously,¹² compound 6 was obtained. After N-tritylation, compound 7 was obtained; however, in our hands, the yield was poor and an alternative route was employed. Removal of the benzyl-protecting group of compound 5 and N-tritylation afforded compound 7; the yield was 41.5% from compound 3. Silyl deprotection with tetra-*n*-butylammonium fluoride (TBAF) gave pip-U monomer 8. The conformations of compound 5 and its morpholino analogue are similar, as confirmed by X-ray crystallographic data (Figure S1A of the Supporting Information).

To convert U to C, the triazole-substituted U moiety of compound 7 was converted to compound 9 by treatment with aqueous NH_4OH solution at room temperature. Acetyl protection of exocyclic amine followed by silyl deprotection of compound 10 by TBAF gave the pip-C monomer 11 in 60% yield from compound 5 (Scheme 2).

For the synthesis of pip-A monomer, compound 1 was treated with 5-amino-4,6-dichloropyrimidine, resulting in selective replacement of one chlorine to yield compound 12.

Scheme 2. Synthesis of Pip-C Monomer 11

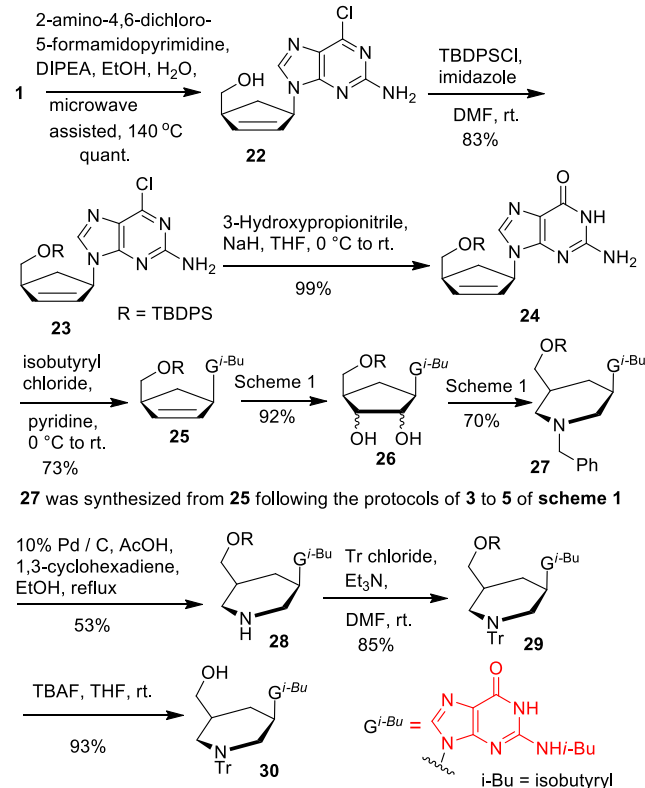
Compound 12 was then converted to compound 13 via the construction of an imidazole ring through a reaction with triethylorthoformate. The OH of compound 13 was protected with *tert*-butyldiphenylsilyl (TBDPS) to yield compound 14. Dihydroxylation of the olefin afforded diol 15 as a mixture of *lyxo* and *ribo* isomers that were then converted to *N*-benzylpiperidine 16. Subsequent treatment with NH_4OH gave compound 17 (Scheme 3). Next, the exocyclic NH₂ of

Scheme 3. Synthesis of Pip-A Monomer 21

compound 17 was protected with a benzoyl group to obtain compound 18. For hydrogenation of compound 18, various conditions were evaluated because the loss of the *N*-benzoyl group was observed (Table S1 of the Supporting Information). The desired product 19 was eventually obtained in 55% yield. Subsequent N-tritylation followed by silyl deprotection provided pip-A monomer 21 in 11% yield from compound 1 (Scheme 3).

For the synthesis of the pip-G monomer, we constructed the 2-amino-6-chloropurine ring through the condensation of compound 1 and 2-amino-4,6-dichloro-5-formamido-pyrimidine to obtain 2-amino-6-chloropurine carbocycle 22 (Scheme 4). Silyl protection of the OH yielded compound 23, which was treated with the sodium salt of 3-hydroxypropionitrile, converting amino-chloropurine to the guanine ring of compound 24. The exocyclic amine was protected with isobutryl amide to provide compound 25. The protocol used for synthesis of the pip-U monomer yielded the trityl-protected pip-G monomer 30 in 17% yield from compound 1. Crystal structures of monomer intermediates (panels B–F of Figure S1 of the Supporting Information) confirmed that the desired configurations were obtained Figure S1.

We next synthesized the chlorophosphoramidate monomers necessary for the synthesis of PPOs (Table 1). Our initial attempts to synthesize the chlorophosphoramidate monomers using LiBr/1,8-diazabicyclo[5.4.0]undec-7-ene (DBU)¹² or 5-(ethylthio)-1*H*-tetrazole (ETT)¹³ methods were not successful, with products obtained in less than 10% yield. We therefore performed the reaction in the presence of strong

Scheme 4. Synthesis of Pip-G Monomer 30**Table 1. Synthesis of Chlorophosphorodiamide Piperidino Monomers^a**

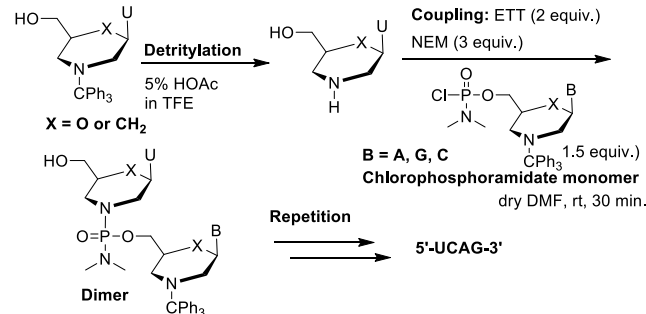
Piperidino monomers		Chlorophosphorodiamide piperidino monomers	
entry	monomer	base	isolated yield (%)
1	U	NaH	20
2	U	LiHMDS	22
3	U	LDA	51/20 ^b
4	C ^{Ac}	NaH	36
5	C ^{Ac}	LDA	49
6	A ^{Bz}	LDA	47
7	G ^{i-Bu}	LDA	35

^aConditions: piperidino monomer (1 equiv), base (3 equiv), and N,N-dimethylphosphoramic dichloride (3 equiv) in dry tetrahydrofuran (THF) at -20 °C for 30 min. ^bThe reaction was performed at -78 °C.

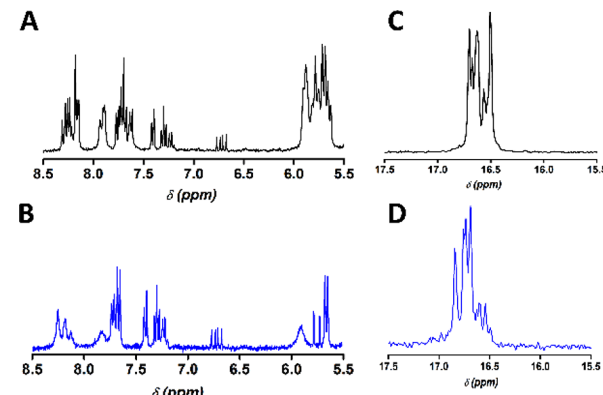
bases at -20 °C to prevent product decomposition. When NaH was used as a base at a temperature of -20 °C, pip-U and pip-C monomers were obtained in 20 and 36% yield, respectively. Although the reaction worked well in the presence of LiHMDS as reported earlier,¹⁴ use of lithium diisopropylamide (LDA) resulted in better yields. At -78 °C using LDA, the reaction was very slow and the yield was approximately 20%. By comparison, at -20°C, the yield of the desired product was 51% and a side product with additional

attachment of chlorophosphoramidate to C=O of U was isolated in 10% yield.

We next synthesized a PMO and PPO with the sequence 5'-UCAG-3' in solution phase (Scheme 5 and Scheme S1 of the

Scheme 5. Solution-Phase Synthesis of Tetramer PMO and PPO

Supporting Information). In the ¹H and ³¹P nuclear magnetic resonance (NMR) spectra of the PMO and PPO tetramers, numbers, multiplicities, and distributions of peaks were similar. ¹H aromatic signals expected from C5 and C6 of pyrimidines and from C8 of G and C8 and C2 of A were observed, indicating that the chemical environments are similar for these protons in PMO and PPO (Figure 2, panels A and B). ³¹P

**Figure 2.** (A) Nucleobase ¹H NMR (300 MHz, CD₃OD) of PMO. (B) Nucleobase ¹H NMR (300 MHz, CD₃OD) of PPO. (C) ³¹P NMR (243 MHz, DMSO-*d*₆) of PMO. (D) ³¹P NMR (243 MHz DMSO-*d*₆) of PPO.

NMR multiplicities arising from eight diastereomeric compounds were also identical for PMO and PPO (Figure 2, panels C and D). High-performance liquid chromatography (HPLC) and matrix-assisted laser desorption/ionization (MALDI) analyses confirmed purities and identities (Figures S2 and S3 of the Supporting Information). Reversed-phase HPLC analyses on a C18 column indicated that the PPO tetramer was more hydrophobic than the PMO tetramer (Figure 3A) as expected because the four oxygen atoms are replaced with CH₂ groups. Thus, PPO may have enhanced cellular uptake and pharmacokinetics compared to PMO.

To evaluate the chemical stability of PPO and PMO in acidic solution, we dissolved the tetramers in formate buffer at pH 2.5 or acetate buffer at pH 5. After 12 h, reverse-phase HPLC analyses showed that the PPO was more stable than the PMO at pH 5 (Figure 3B and Figure S4 of the Supporting

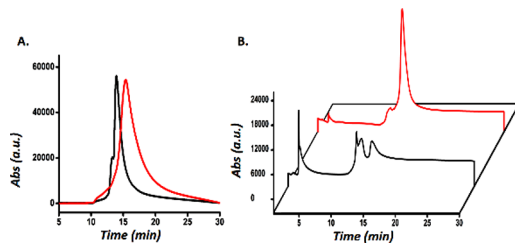


Figure 3. (A) Reverse-phase HPLC chromatograms of PMO (black) and PPO (red) tetramers to evaluate polarity. (B) Reverse-phase HPLC chromatograms of PMO (black) and PPO (red) after 12 h at pH 5.

Information), implying that the PPO will be more stable in endosomolytic compartments than the PMO. Both oligomers were degraded to unidentified fragments at pH 2.5 (Figure S5 of the Supporting Information).

We next used a combination of manual (Scheme S2 of the Supporting Information) and automated (Scheme S3 of the Supporting Information) solid-phase synthesis to synthesize oligomers as per our previous method¹³ that contained both PMO and PPO residues (Table 2). The piperidino

Table 2. Sequences and Thermal Melting Temperatures (T_m) of Duplexes of PMOs and PMO–PPO Chimeras with DNA and RNA^a

ID	Sequence (5 to 3) ^b	T_m with	ΔT_m	T_m with	ΔT_m
		DNA	(°C) ^c	RNA	(°C) ^c
ON1	TTTACTCACAT	26.0		24.0	
ON2	TTGTACTCACAT	37.0		40.4	
ON3	TTUTACTCACAT	22.1	-3.9	28.0	+4.0
ON4	TTUTACTCACAT	20.7	-5.3	28.5	+4.5
ON5	TTTACUCACAT	12.5	-13.5	17.5	-6.5
ON6	TTUTACTCACAT	24.0	-2.0	29.8	+5.8
ON7	TTGTACTCACAT	32.2	-4.8	38.0	-2.4
ON8	TTGTACTCACAT	35.0	-2.0	40.1	-0.3
ON9	TTGTACTCACAT	32.5	-4.5	38.9	-1.5
ON10	TTGTACUCACAT	26.3	-10.7	26.7	-13.7

^aConditions: 40 mM phosphate buffer (pH 7), with 2 μ M for each strand. T_m values reported are the averages of two independent experiments that were within $\pm 0.5^\circ$. ^bBlue letters indicate PMO, and red letters indicate PPO. ^cThe ΔT_m values are relative to T_m of the duplex formed between ON1 or ON2 and complementary RNA or DNA.

chlorophosphoramidate monomers were incorporated manually. The coupling efficiency for piperidino chlorophosphoramidate monomers was an average of 95% as per the trityl assay. Yield and purity were determined using HPLC and MALDI (Table S2 and Figures S6–S14 of the Supporting Information).

Incorporation of one or two piperidinomonomers destabilized the duplex with DNA by 2–13.5 °C compared to the duplexes formed with PMO (Table 2 and Figures S15–S24 of the Supporting Information). The destabilization increased when a piperidino was incorporated in the middle (ON5 and

ON10). In the case of RNA, the T_m value of the duplex of the oligomer with one pip-A residue was comparable to that of PMO (ON8). Interestingly, chimeras with pip-U or pip-C at the 3' or 5' end or both termini (ON3, ON4, and ON6) had higher T_m values than the corresponding PMO. The pip-G-containing chimera (ON7) and the chimera with both pip-G and pip-A (ON9) had T_m values that were lower by 2.4 and 1.5 °C, respectively, than that of the PMO–RNA duplex. In the case of the oligomer with four PPO residues (ON10), the T_m of the duplex with RNA was 13.7 °C lower than the T_m of the duplex with PMO. We are in the process of making uniform piperidino oligomers to understand the differences noted between PMO and PPO in binding to DNA and RNA.

In the CD spectra of duplexes with DNA, there was a strong positive band at around 275 nm and a negative band at around 210 nm, which is characteristic of a B-form conformation. Even the duplex between the oligomer with four piperidino substitutions and DNA appears to have a global conformation similar to that of the PMO:DNA duplex, as shown by similarities of CD spectra (Figure S25 of the Supporting Information). In the case of duplexes with RNA, the CD spectra of duplexes formed with oligomers with one or two pip-U or pip-C residues (ON3, ON4, ON5, and ON6) were similar to that of the duplex of PMO (ON1) with RNA (Figure S26 of the Supporting Information). Although ON2 differs by only substitution of PMO T by PMO G at the third position with respect to ON1, the CD spectrum of the duplex with RNA was significantly different than that of the duplex formed by the PMO ON1 with RNA (Figure S27 of the Supporting Information). Duplexes between RNA and oligomers with pip-G (ON7, ON8, ON9, and ON10) and with the PMO (ON2) and RNA had similar CD spectra (Figure S26 of the Supporting Information). The positive bands at around 260 and 280 nm were suggestive of structural properties of a conformation in between B- and A-form helices.

Finally, to study the effect of incorporation of PMO or PPO into a RNA duplex, we modeled the structures of a RNA duplex containing a single modification of either PMO or PPO. The crystal structure of the octamer duplex [CGAA(dT)-UCG]₂ with a single 2'-deoxythymidine per strand served as the template [Protein Data Bank (PDB) ID 5DEK].¹⁵ The dT in one strand was removed, and the PMO or PPO residue was manually built into the RNA backbone in UCSF Chimera,¹⁶ using an all-equatorial conformation for the six-membered rings. Both models were energy-minimized with the program AMBER¹⁷ using Amber-14 parameters (<https://ambermd.org/>). There was a virtually seamless fit of PMO and PPO monomers inside an RNA backbone (Figure 4). This analysis points out that both PMO and PPO would fit into other chimeric oligonucleotides targeting RNA using different

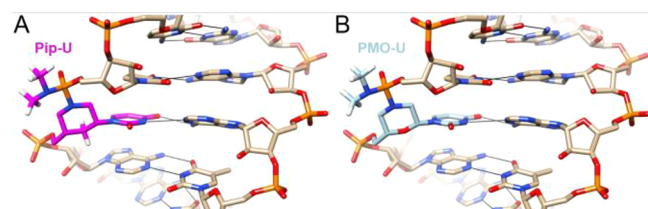


Figure 4. Models of a RNA duplex containing (A) pip-U and (B) PMO-U monomers generated with the program UCSF Chimera.

mechanisms of action, such as RNase-H-based antisense and Argonaute-2-based RNAi therapeutics.

In summary, we have synthesized piperidino monomer building blocks and incorporated these residues using a solid-phase synthesis protocol into the PMO backbone to generate PMO–PPO chimeras. The stabilities of duplexes between DNA and PMO–PPO chimeras was lower than that of the DNA:PMO duplex. Incorporation of one or two pip-A, pip-U, or pip-C residues resulted in either comparable or higher duplex stability with RNA; however, multiple piperidino monomers destabilized the hybrid duplexes. Although stability of duplexes is one requirement for therapeutic applications of oligonucleotide-based drugs, other parameters, such as metabolic stability, cell permeation, release from the endolysosomal compartments, and target specificity, are also critical. Given the data reported here, further evaluation of the gene-silencing and splice-modulating activities of PMO–PPO chimeric oligomers in the context of both antisense and RNA interference is warranted.

■ ASSOCIATED CONTENT

Data Availability Statement

Data are available in the published article and its [Supporting Information](#).

⑤ Supporting Information

The Supporting Information is available free of charge at <https://pubs.acs.org/doi/10.1021/acs.orglett.2c04067>.

Experimental procedures, compound characterization, and description of the procedures ([PDF](#))

Accession Codes

CCDC 2202900–2202902, 2202923, and 2202926 contain the supplementary crystallographic data for this paper. These data can be obtained free of charge via www.ccdc.cam.ac.uk/data_request/cif, or by emailing data_request@ccdc.cam.ac.uk, or by contacting The Cambridge Crystallographic Data Centre, 12 Union Road, Cambridge CB2 1EZ, UK; fax: +44 1223 336033.

■ AUTHOR INFORMATION

Corresponding Authors

Muthiah Manoharan – *Alnylam Pharmaceuticals, Cambridge, Massachusetts 02142, United States;* orcid.org/0000-0002-7931-1172; Email: mmanoharan@alnylam.com

Surajit Sinha – *School of Applied and Interdisciplinary Sciences, Indian Association for the Cultivation of Science, Kolkata 700032, India;* orcid.org/0000-0001-8884-1194; Email: ocss5@iacs.res.in

Authors

Atanu Ghosh – *School of Applied and Interdisciplinary Sciences, Indian Association for the Cultivation of Science, Kolkata 700032, India*

Masaaki Akabane-Nakata – *Alnylam Pharmaceuticals, Cambridge, Massachusetts 02142, United States*

Jayanta Kundu – *School of Applied and Interdisciplinary Sciences, Indian Association for the Cultivation of Science, Kolkata 700032, India*

Joel M. Harp – *Department of Biochemistry, School of Medicine, Vanderbilt University, Nashville, Tennessee 37232, United States*

Mimouna Madaoui – *Alnylam Pharmaceuticals, Cambridge, Massachusetts 02142, United States*

Martin Egli – *Department of Biochemistry, School of Medicine, Vanderbilt University, Nashville, Tennessee 37232, United States;* orcid.org/0000-0003-4145-356X

Complete contact information is available at:
<https://pubs.acs.org/10.1021/acs.orglett.2c04067>

Author Contributions

[†]Atanu Ghosh and Masaaki Akabane-Nakata contributed equally to this work.

Notes

The authors declare no competing financial interest.

■ ACKNOWLEDGMENTS

Surajit Sinha thanks the Science and Engineering Research Board (SERB), New Delhi, Government of India (Grant TTR/2021/000044), for grant support and the Technical Research Center (TRC) facility at Indian Association for the Cultivation of Science (IACS) for use of a DNA synthesizer. Jayanta Kundu and Atanu Ghosh thank the Council of Scientific and Industrial Research (CSIR) for their fellowships.

■ REFERENCES

- (1) (a) Summerton, J. E. *Biochim. Biophys. Acta* **1999**, *1489*, 141–158. (b) Summerton, J. E.; Weller, D. *Antisense Nucleic Acid Drug Dev.* **1997**, *7*, 187–195. (c) Summerton, J. E. *Methods Mol. Biol.* **2017**, *1565*, 1–15.
- (2) (a) Burlina, F.; Favre, A.; Fourrey, J.-L.; Thomas, M. *Chem. Commun.* **1996**, 1623–1624. (b) Bessières, M.; Chevrier, F.; Roy, V.; Agrofoglio, L. A. *Future Med. Chem.* **2015**, *7*, 1809–1828. (c) Akabane-Nakata, M.; Chickering, T.; Harp, J. M.; Schlegel, M. K.; Matsuda, S.; Egli, M.; Manoharan, M. *Org. Lett.* **2022**, *24*, S25–S30. (d) Akabane-Nakata, M.; Kumar, P.; Das, R. S.; Erande, N. D.; Matsuda, S.; Egli, M.; Manoharan, M. *Org. Lett.* **2019**, *21*, 1963–1967.
- (3) (a) Duan, D.; Goemans, N.; Takeda, S.; Mercuri, E.; Aartsma-Rus, A. *Nat. Rev. Dis. Primers* **2021**, *7*, 13. (b) Li, D.; Adams, A. M.; Johnsen, R. D.; Fletcher, S.; Wilton, S. D. *Mol. Ther. Nucleic Acids* **2020**, *22*, 263–272. (c) Moumné, L.; Marie, A.-C.; Crouvezier, N. *Pharmaceutics* **2022**, *14* (2), 260.
- (4) Nan, Y.; Zhang, Y.-J. *Front. Microbiol.* **2018**, *9*, 750.
- (5) Devi, G. R.; Beer, T. M.; Corless, C. L.; Arora, V.; Weller, D. L.; Iversen, P. L. *Clin. Cancer Res.* **2005**, *11*, 3930–3938.
- (6) (a) Łukasik, B.; Mikina, M.; Mikołajczyk, M.; Pawłowska, R.; Zurawński, R. *RSC Adv.* **2020**, *10*, 31838–31847. (b) O'Dwyer, P. J.; Shoemaker, D. D.; Jayaram, H. N.; Johns, D. G.; Cooney, D. A.; Marsoni, S.; Malspeis, L.; Plowman, J.; Davignon, J. P.; Davis, R. D. *Invest. New Drugs* **1984**, *2*, 79–84. (c) Marquez, V. E. Carbocyclic nucleosides. In *Advances in Antiviral Drug Design*; De Clercq, E., Ed.; Elsevier: Amsterdam, Netherlands, **1996**; Vol. 2, pp 89–146, DOI: [10.1016/S1075-8593\(96\)80104-3](https://doi.org/10.1016/S1075-8593(96)80104-3). (d) Štambaský, J.; Hocek, M.; Kočovský, P. *Chem. Rev.* **2009**, *109*, 6729–6764.
- (7) Amantana, A.; Iversen, P. L. *Curr. Opin. Pharmacol.* **2005**, *5*, 550–555.
- (8) Langner, H. K.; Jastrzebska, K.; Caruthers, M. H. *J. Am. Chem. Soc.* **2020**, *142*, 16240–16253.
- (9) (a) Pattanayak, S.; Khatra, H.; Saha, S.; Sinha, S. *RSC Adv.* **2014**, *4*, 1951–1954. (b) Paul, S.; Pattanayak, S.; Sinha, S. *Tetrahedron Lett.* **2014**, *55*, 1072–1076. (c) Nandi, B.; Khatra, H.; Khan, P. P.; Bhadra, J.; Pattanayak, S.; Sinha, S. *ChemistrySelect* **2017**, *2*, 5059–5067. (d) Kundu, J.; Das, U.; Bose, C.; Bhadra, J.; Sinha, S. *BioRxiv* **2021**, *06.04.447039*.
- (10) Palframan, M. J.; Alharthy, R. D.; Powalowska, P. K.; Hayes, C. J. *Org. Biomol. Chem.* **2016**, *14*, 3112–3119.

- (11) Debreczeni, N.; Bege, M.; Herczeg, M.; Bereczki, I.; Batta, I.; Herczegh, P.; Borbás, A. *Org. Biomol. Chem.* **2021**, *19*, 8711–8721.
- (12) Bhadra, J.; Pattanayak, S.; Sinha, S. *Curr. Protoc. Nucleic Acid Chem.* **2015**, *62*, 4.65.1–4.65.26.
- (13) Kundu, J.; Ghosh, A.; Ghosh, U.; Das, A.; Nagar, D.; Pattanayak, S.; Ghose, A.; Sinha, S. *J. Org. Chem.* **2022**, *87*, 9466–9478.
- (14) Shestopalov, I. A.; Sinha, S.; Chen, J. K. *Nat. Chem. Biol.* **2007**, *3*, 650–651.
- (15) Kel'in, A. V.; Zlatev, I.; Harp, J. M.; Jayaraman, M.; Bisbe, A.; O'Shea, J.; Taneja, N.; Manoharan, R. M.; Khan, S.; Charisse, K.; Maier, M. A.; Egli, M.; Rajeev, K. G.; Manoharan, M. *J. Org. Chem.* **2016**, *81*, 2261–2279.
- (16) Pettersen, E. F.; Goddard, T. D.; Huang, C. C.; Couch, G. S.; Greenblatt, D. M.; Meng, E. C.; Ferrin, T. E. *J. Comput. Chem.* **2004**, *25*, 1605–1612.
- (17) Case, D. A.; Cheatham, T. E., 3rd; Darden, T.; Gohlke, H.; Luo, R.; Merz, K. M., Jr; Onufriev, A.; Simmerling, C.; Wang, B.; Woods, R. *J. J. Comput. Chem.* **2005**, *26*, 1668–1688.

□ Recommended by ACS

A Predictably Selective Palladium-Catalyzed Aliphatic C–H Oxygenation

Dmitry P. Lubov, Konstantin P. Bryliakov, *et al.*

FEBRUARY 24, 2023
ORGANIC LETTERS

READ

Covalent Tethers for Precise Amino Alcohol Syntheses: Ring Opening of Epoxides by Pendant Sulfamates and Sulfamides

Someshwar Nagamalla, Shyam Sathyamoorthi, *et al.*

FEBRUARY 06, 2023
ORGANIC LETTERS

READ

Syntheses of Base-Labile Pseudo-Complementary SNA and L- α TNA Phosphoramidite Monomers

Fuminori Sato, Hiroyuki Asanuma, *et al.*

JANUARY 06, 2023
THE JOURNAL OF ORGANIC CHEMISTRY

READ

Expansion of Phosphoramidite Chemistry in Solid-Phase Oligonucleotide Synthesis: Rapid 3'-Dephosphorylation and Strand Cleavage

Kazuki Yamamoto, Yoshiyuki Hari, *et al.*

FEBRUARY 22, 2023
THE JOURNAL OF ORGANIC CHEMISTRY

READ

[Get More Suggestions >](#)